The high-energy gamma-ray spectra of TeV blazars

Deivid Ribeiro[a,b,*] **for the VERITAS Collaboration**

[a] *School of Physics & Astronomy, 116 Church St SE, Minneapolis, USA*

[b] *Minnesota Institute for Astrophysics, 116 Church St SE, Minneapolis, USA*

E-mail: ribei056@umn.edu

Blazars are a subclass of active galactic nuclei with relativistic jets pointed toward the observer, emitting non-thermal, high-energy gamma rays that can exceed 1 TeV. The underlying mechanism for the emission of these gamma rays is evident in the observed spectral energy distribution (SED), which is modeled to include the underlying particle populations, and acceleration and cooling mechanisms in the jets. The *Fermi*-LAT is a space-based telescope sensitive to gamma rays with energies from 50 MeV to 1 TeV and VERITAS is a ground-based observatory that detects VHE gamma rays from 85 GeV to 30 TeV. We use data from the *Fermi*-LAT and VERITAS to study a sample of TeV blazars, exploiting more than ten years of data from both instruments to construct a rich population of the flux distributions. Temporal and spectral analyses were conducted on a sample of eight high-frequency-peaked BL Lac objects (HBLs), a subclass of blazars that have their synchrotron peak at frequencies between 10^{15} Hz and 10^{17} Hz. We used Bayesian blocks to define periods with steady flux and accounted for the absorption effect from the extragalactic background light (EBL). We report on the distribution of spectral fluxes, particularly focusing on the properties of the spectral cutoff in the SED through various flux states.

---

[*]Speaker

1. Introduction

Blazars, a distinct subclass within active galactic nuclei (AGN), are believed to have relativistic jets that align with the observer at small angles, emitting gamma rays that can exceed 1 TeV. Understanding the mechanisms behind these high-energy gamma rays involves analyzing the spectral energy distribution (SED) with models of the particle populations including the acceleration and cooling processes in the relativistic jets.

In the taxonomy of blazars, high-frequency-peaked BL Lac objects (HBLs) stand out. With a synchrotron peak occurring at frequencies surpassing 10^{15} Hz, particularly within the UV/X-Ray spectrum, HBLs display an emission profile suggesting synchrotron radiation from a dynamically accelerated population of charged particles within the jet framework. Investigating HBLs enhances our understanding of blazar physics, contributing significantly to unraveling the complexities intrinsic to the cosmic processes associated with active galactic nuclei.

In most cases, VERITAS observations of HBLs are triggered by alerts of bright flares at other wavelengths, leading to observation biases focused on these elevated states. The sources presented here are known HBLs that were selected for monitoring, where the observations were taken at regular intervals to measure a wider range of states regardless of flares. The long-term variability is evident: from the multiple states observed (low, high, flaring, etc.) we can compile the distribution of fluxes to learn about the underlying acceleration and cooling mechanisms. A previous study quantified the distribution of these flux states for multiple sources and carried out modeling studies to find the spectral curvature that provided information on the cooling of the electron population [1]. In this study, we systematically fit spectral models for multiple sources.

2. Methods

2.1 Instruments

The *Fermi*-LAT is a space-based telescope sensitive to gamma rays with energies from 50 MeV to 1 TeV. Given its ability to survey the full sky every 3 hours, it is possible to compile long-term monitoring observations to find time variability over many years [2].

VERITAS is a ground-based observatory that detects VHE gamma rays from 85 GeV to 30 TeV [3]. Although it has $\sim 10^5$ m^2 effective area significantly improving the sensitivity over that of *Fermi*-LAT, it is a pointing telescope where observations must compete for time. Therefore, only small observation windows are available over many years.

2.2 Selection of States During Time Variability

We have compiled the lightcurve data for the 8 sources, 1ES 1011+496, Mrk 421, 1ES 1215+303, MS 1221.8+2452, 1ES 1218+304, Mrk 501, 1ES 1959+650, 1ES 2344+514 over 10 years for this study. Out of these sources, we focus on 1ES 1011+496 as a rich data set to use for a spectral study. We use Bayesian blocks to define periods of steady flux, and reconstructed fluxes are deabsorbed from the EBL [4, 5]. The blocks are calculated for each instrument with a 3σ prior probability. The blocks from each instrument are assumed to be independent, so the unity of all change points were used - this means that all change points are placed on the same timeline, and then the resulting time bins are checked for overlapping states. Between VERITAS and *Fermi*-LAT,

we find the explicitly overlapping states and use data from each instrument to calculate SEDs for that block.

3. Results

3.1 Light Curve
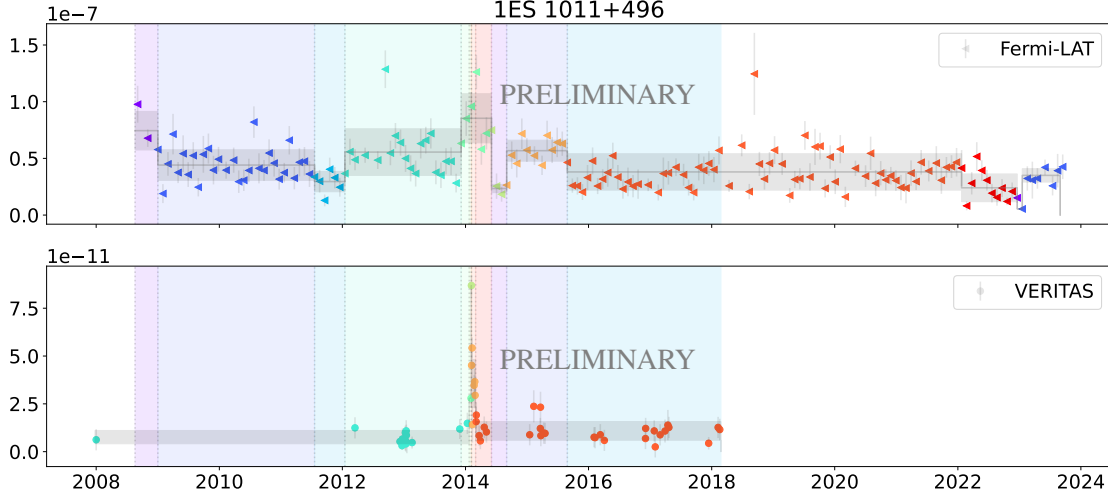
Figure 1: Light curve of 1ES1011+496. Grey shaded regions indicate block per instrument, while colored shading indicates overlapping blocks. Explicitly overlapping blocks occur between 2012 and 2018. There are several small blocks within the fast changing flare period in 2014.

Figure 1 shows the lightcurve of 1ES 1011+496, where the Bayesian block algorithm of section 2.2 is used to demark the separate states. There were 8 overlapping states where simultaneous observations were taken by both instruments, including the high cadence observations during the flare period in 2014. The observations before and after the flare are critical to measuring different states of this HBL.

3.2 SEDs

After selecting the observation periods with the largest overlap between both instruments, each was analyzed independently to create a combined SED. The SEDs are fit with power law (PWL), log parabola (LP), exponential cutoff power law (ECPL), and Super ECPL (SECPL). Since the redshift of 1ES 1011+496 is known ($z = 0.212$), the effects of the EBL absorption [4] on each flux point are removed to find the intrinsic spectrum in each time period, shown in all the SEDs in Figure 2. The curved models (LP, ECPL, SECPL) are compared to PWL using the Akaike Information Criterion $\texttt{AIC} = k - \ln L$ where k is the number of free parameters and L is the likelihood. The smallest $\Delta_{AIC} = \texttt{AIC}_{curved} - \texttt{AIC}_{PWL}$ indicates a better fit [6].

In some cases, curvature is preferred ($\Delta_{AIC} < 10$), which may indicate that models with suppressed TeV emission are preferred. These values are summarized in Table 1, where bins 4, 11 and 12 show a preference for the log parabola model over the power law.
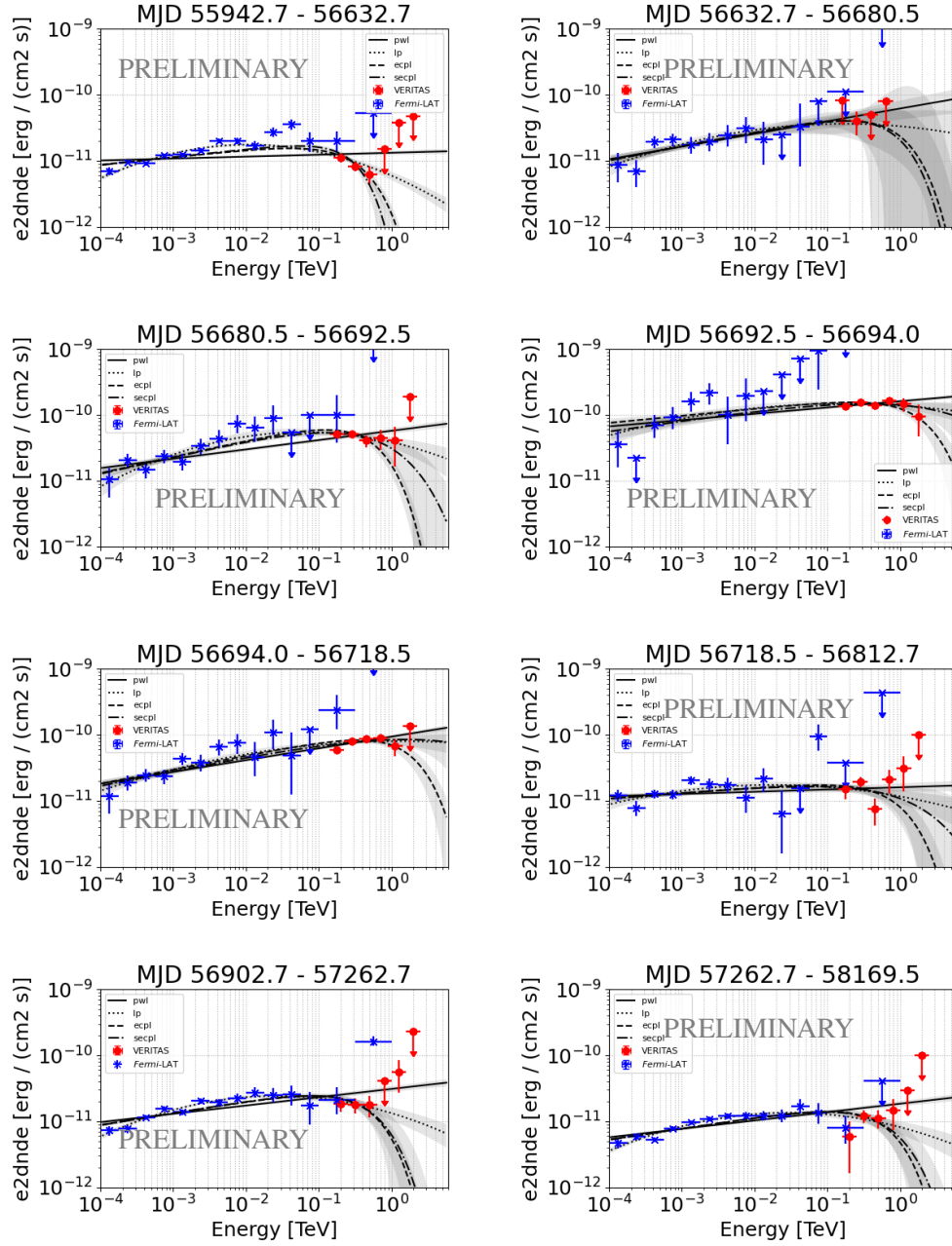
Figure 2: Spectra for each of the overlapping light curve bins of 1ES 1011+496. Blocks 4, 11 and 12 (SEDs top left, bottom left and bottom right), appear to show preference for a curved model with ($\Delta_{AIC} < 10$).

Table 1: The ΔAIC between the curved models log parabola (LP), exponential cut-off powerlaw (ECPL) and super exponential cut-off power law (SECPL) for 1ES 1011+496 for each time period analyzed. For this source, 16 bins were created defined by the independent Bayesian blocks; however, only bins 4-12 overlapped between VERITAS and *Fermi*-LAT. Bins 4,11 and 12 show significantly different AIC values $\Delta_{AIC} < 10$, indicating a preference for the curved spectral models against a power law.

Bin	Start (MJD)	End (MJD)	ΔAIC_{LP}	ΔAIC_{ECPL}	ΔAIC_{SECPL}
4	55942.7	56632.7	-89.9	-67.2	-74.5
5	56632.7	56680.5	0.4	1.5	-0.6
6	56680.5	56692.5	-6.2	-3.1	-7.1
7	56692.5	56694.0	-1.9	3.3	-3
8	56694.0	56718.5	-1.2	4.2	-1.5
9	56718.5	56812.7	-2.2	0.3	-2.2
11	56902.7	57262.7	-36.3	-16.6	-20.1
12	57262.7	58169.5	-33.3	-14.3	-18.1

4. Discussion

In the case of synchrotron self-Compton (SSC) model emission, it can be shown [7] that there is a relationship between the photon and electron spectral cutoff sharpness or index. The acceleration and radiative cooling of the electrons leads to synchrotron photons that Compton scatter directly with the same population of electrons. The resulting gamma-ray spectrum is typically described by a curved model, such as a power-law with an exponential cutoff

$$\frac{dN}{dE} = N_0 \left(\frac{E}{E_0}\right)^{-\Gamma} \exp\left[-\left(\frac{E}{E_C}\right)^{\alpha}\right] \tag{1}$$

The cutoff energy E_C and index α are set by the interplay between the acceleration and cooling mechanisms of the parent electron particles and target photon field. This curvature is also affected by the cross-section of the interaction, which are either in the Thomson or Klein-Nishina regimes. For the higher energy Klein-Nishina regime, the electron is expected to transfer nearly all of its energy to the photon, leading to a Compton spectrum resembling the curvature of the synchrotron spectrum where $\beta_E = \alpha$ for electron cutoff index β_E and photon cut-off index α.

In the cases where the curvature of the VHE spectrum is sub-exponential ($\alpha < 1$), the photon cutoff index α can indicate the electron cutoff index β_E [7, 8]

$$\beta_E = \frac{4\alpha}{1 - \alpha} \tag{2}$$

where a Thomson regime is assumed in the SSC model.

In Table 1, in the blocks where the SECPL model is a good fit (where $\Delta_{AIC} < 10$, blocks 4, 11 and 12), we test that the particles are in the Thomson regime by measuring $\alpha \simeq 0.4 \pm 0.2$, corresponding to a steep electron cutoff $\beta_E \simeq 3 \pm 2$. The observed high-energy gamma-ray data are useful in constraining models and for deriving the shape of the electron cutoff energy which, in turn, can provide insights on particle acceleration processes in the blazar jet.

References

[1] Q. Feng, *Exploring the High-Energy Gamma-Ray Spectra of TeV Blazars*, in *Proceedings of 37th International Cosmic Ray Conference — PoS(ICRC2021)*, p. 802, July, 2021, DOI [2108.05333].

[2] W.B. Atwood, A.A. Abdo, M. Ackermann, W. Althouse, B. Anderson, M. Axelsson et al., *The Large Area Telescope on the Fermi Gamma-Ray Space Telescope Mission*, *Astrophysical Journal* **697** (2009) 1071.

[3] T. Weekes, H. Badran, S. Biller, I. Bond, S. Bradbury, J. Buckley et al., *VERITAS: The Very Energetic Radiation Imaging Telescope Array System*, *Astroparticle Physics* **17** (2002) 221.

[4] A. Domínguez, J.R. Primack, D.J. Rosario, F. Prada, R.C. Gilmore, S.M. Faber et al., *Extragalactic Background Light Inferred from AEGIS Galaxy-SED-type Fractions*, *Monthly Notices of the Royal Astronomical Society* **410** (2011) 2556.

[5] J.D. Scargle, J.P. Norris, B. Jackson and J. Chiang, *Studies in Astronomical Time Series Analysis. VI. Bayesian Block Representations*, *The Astrophysical Journal* **764** (2013) 167.

[6] H. Akaike, *A New Look at the Statistical Model Identification*, *IEEE Transactions on Automatic Control* **19** (1974) 716.

[7] E. Lefa, S.R. Kelner and F.A. Aharonian, *On the Spectral Shape of Radiation Due to Inverse Compton Scattering Close to the Maximum Cutoff*, *The Astrophysical Journal* **753** (2012) 176.

[8] C. Romoli, A. Taylor and F. Aharonian, *Cut-off Characterisation of Energy Spectra of Bright Fermi Sources: Current Instrument Limits and Future Possibilities*, *Astroparticle Physics* **88** (2017) 38.

PoS(HEPROVII)075